

Surface morphology, structural and optical properties of polar and non-polar ZnO thin films: A comparative study

R. Deng^a, B. Yao^{a,b,*}, Y.F. Li^b, B.H. Li^b, Z.Z. Zhang^b, H.F. Zhao^b, J.Y. Zhang^b, D.X. Zhao^b, D.Z. Shen^b, X.W. Fan^b, L.L. Yang^c, Q.X. Zhao^c

^a Department of Physics, Jilin University, Changchun 130023, People's Republic of China

^b Key Laboratory of Excited State Processes, Changchun Institute of Optics, Fine Mechanics and Physics, Chinese Academy of Sciences, Changchun 130033, People's Republic of China

^c Department of Science and Technology (ITN), Linköping University, Sweden

ARTICLE INFO

Article history:

Received 25 May 2009

Received in revised form

29 June 2009

Accepted 31 July 2009

Communicated by H. Asahi

Available online 11 August 2009

PACS:

81.15.Hi

78.55.Et

78.66.Hf

Keywords:

A1. X-ray diffraction

A1. Atomic force microscopy

A1. Photoluminescence

A3. Molecular beam epitaxy

B1. Zinc oxide

ABSTRACT

The polar and non-polar ZnO thin films were fabricated on cubic MgO (111) and (001) substrates by plasma-assisted molecular beam epitaxy. Based on X-ray diffraction analysis, the ZnO thin films grown on MgO (111) and (100) substrates exhibit the polar *c*-plane and non-polar *m*-plane orientation, respectively. Comparing with the *c*-plane ZnO film, the non-polar *m*-plane ZnO film shows cross-hatched stripes-like morphology, lower surface roughness and slower growth rate. However, low-temperature photoluminescence measurement indicates the *m*-plane ZnO film has a stronger 3.31 eV emission, which is considered to be related to stacking faults. Meanwhile, stronger band tails absorbance of the *m*-plane ZnO film is observed in optical absorption spectrum.

© 2009 Elsevier B.V. All rights reserved.

1. Introduction

Zinc oxide (ZnO) is an important wide band gap semiconductor material due to its use in a wide variety of applications such as ultraviolet (UV), light emitting devices (LEDs), laser diodes (LDs) and photodetectors [1–3]. The main advantages of ZnO are a wide direct band gap (3.37 eV) and a large exciton binding energy (60 meV). Due to the large exciton binding energy than GaN (25 meV), ZnO has better lasing efficiency than GaN [4]. However, before ZnO achieves its commercial application, there still remain some problems to be solved, such as the surface smoothness, reproducibility of its p-type doping, and how to enhance its inner quantum efficiency. Because ZnO has no inversion symmetry, ZnO crystal along the *c*-axis has alternate zinc ion layers with oxygen

ion layers, which cause polarization along the *c*-axis. Generally, the electric field induced by polarization has negative effects on optical and electrical properties of devices [5]. For instance, a decrease in the overlapping of the electron and hole wave function in the quantum well will result in a decrease of internal quantum efficiency of the LEDs and LDs [6–8]. Therefore, advantages of non-polar growth include improved optical efficiency for quantum wells [9,10] and in-plane piezoelectric effects. To eliminate the polarization effects, it is necessary to grow ZnO films without polarity along the growth direction, such as growth of non-polar films. There are several reports on growing non-polar *a*-plane ZnO on *r*-plane sapphire, *m*-plane ZnO on *m*-plane sapphire, and *m*-plane ZnO on (001) MgO [11–15]. But the research on properties of *m*-plane ZnO thin films is seldom reported, especially for the study comparing with polar ZnO film.

In this paper, surface morphology, optical and photoluminescent properties of polar and non-polar ZnO thin films have been comparatively investigated by scanning electron microscopy (SEM), atom force microscopy (AFM), photoluminescence (PL) and optical absorption spectra.

* Corresponding author at: Key Laboratory of Excited State Processes, Changchun Institute of Optics, Fine Mechanics and Physics, Chinese Academy of Sciences, 3888 East Nan-Hu Road, Changchun 130033, People's Republic of China.

Tel.: +86 431 86176355; fax: +86 431 85682964.

E-mail address: binyao@jlu.edu.cn (B. Yao).

2. Experimental detail

The ZnO thin films were deposited on MgO (111) and (001) substrates by plasma-assisted molecular beam epitaxy (p-MBE) under the same growth condition. O₂ gas was used as O source and activated during the growth process by an Oxford Applied Research Model HD25 rf (13.56 MHz) atomic source. Zinc source and substrate temperatures were fixed at 240 and 750 °C, and the O₂ gas flux was fixed at 0.8 sccm, respectively. During the growth process, the pressure of the chamber was 2×10^{-5} mbar. The electron concentrations of ZnO films grown on MgO (111) and (001) substrates were 1.2×10^{17} and 7.6×10^{17} cm⁻³, and mobility was 15 and 2 cm² V⁻¹ s⁻¹, respectively. The structures of the films were characterized by X-ray diffraction (XRD) with Cu K α_1 radiation ($\lambda = 0.15406$ nm). The low-temperature PL measurement is performed using the 325 nm line of He–Cd laser as an excitation source. The room temperature absorbance measurement was performed using an UV–vis–NIR spectrophotometer (Shimadzu) and electrical properties were measured in the van der Pauw configuration by a Hall-effect measurement system at room temperature. The surface morphologies were observed by AFM and SEM.

3. Results and discussion

Fig. 1 shows XRD θ – 2θ scan patterns of ZnO thin films deposited on cubic MgO (111) and (001) substrates. A (002) preferential orientation (*c*-plane) of ZnO layer is inferred for the ZnO film grown on MgO (111) substrate according to strong peak at 34.56°, as shown in Fig. 1(a). A weak peak at 36.14° is attributed to (101) orientation of ZnO layer. In contrast, the ZnO film grown on MgO (001) substrate shows a strong (100) diffraction peak at 31.68° corresponding to *m*-plane ZnO, as shown in Fig. 1(b). The weak ZnO (002) diffraction peak is believed due to select nucleation sites at particulates or other substrate defects, where

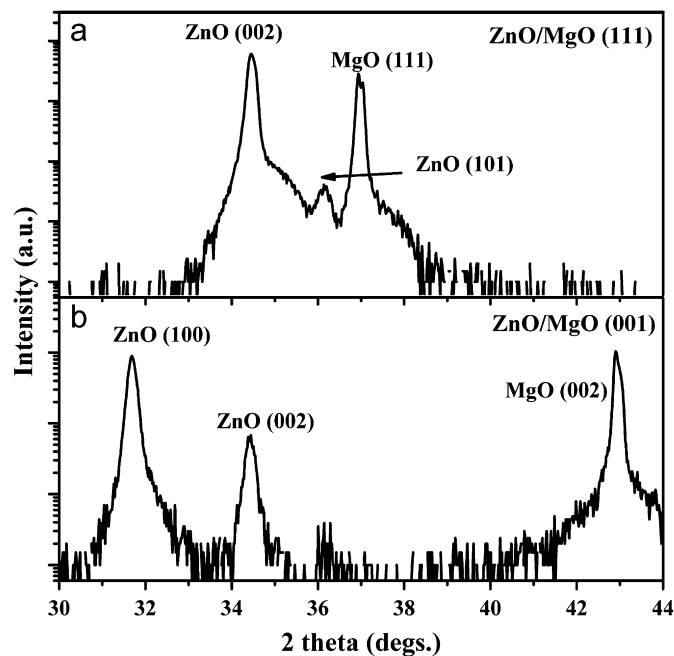


Fig. 1. XRD patterns of ZnO films grown on MgO (a) (111) and (b) (001) substrates.

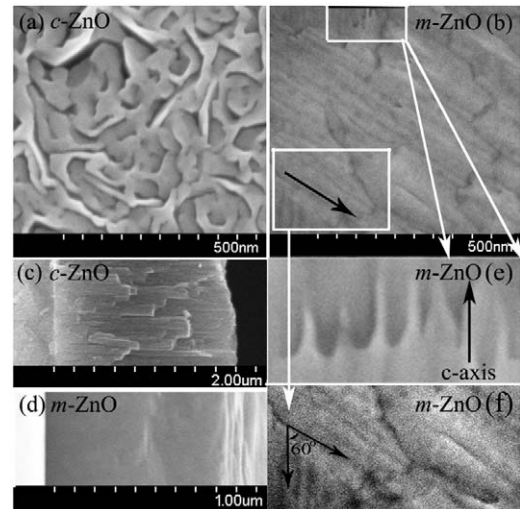


Fig. 2. FESEM surface morphology images of the (a) *c*-plane and (b) *m*-plane ZnO thin films. Cross-section morphology of the (c) *c*-plane and (d) *m*-plane ZnO thin films. (e) and (f) show the enlarged regions in (b).

polycrystalline growth with preferential *c*-axis growth would dominate [11]. In this paper, the ZnO films grown on MgO (111) and (001) substrates are denoted as *c*-ZnO and *m*-ZnO, respectively.

Surface SEM images of the *c*- and *m*-ZnO thin films are shown in Fig. 2(a), (b), (e) and (f). The surface of the *c*-ZnO film exhibits a wall-like morphology, as shown in Fig. 2(a), and the thickness of nanowall is estimated to be in the range 20–50 nm. Based on the XRD result, the orientation of the vertical nanowall is paralleled to *c*-axis. Fig. 2(b) shows the horizontal stripes-like surface morphology of the *m*-ZnO film. The ends of the stripes show tube-like structures, as magnified and shown in Fig. 2(e). The orientation of the stripes, depicted as a black arrow in Fig. 2(b), is believed to be paralleled to *c*-axis from the XRD analysis. Interestingly, the stripes intersect with a cross angle of $\sim 60^\circ$ and form so-called cross-hatched morphology, as shown in Fig. 2(f). The cross-hatched growth mode may introduce defects into the cross points, such as grain boundaries and dislocation, and influence optical properties of the film. This will be discussed later.

Fig. 2(c) and (d) shows cross-sectional SEM morphology of the *c*- and *m*-ZnO thin films. The thickness of the *c*- and *m*-ZnO thin films is estimated to be 1.9 and 0.9 μm , respectively, indicating the growth rate of the *m*-plane ZnO film is much slower than that of *c*-plane ZnO film. Taking the growth time into consideration, the average growth rates are determined to be 15.8 and 7.5 nm/min for the *c*- and *m*-ZnO films, respectively. It is well known that the growth rate is related to surface energy, for example, high surface energy means fast growth rate [16]. The surface energy of ZnO (001) plane is higher than that of ZnO (100) plane, responsible for the fast growth rate of ZnO (001) plane in the present experiment. Sun et al. also had observed similar phenomenon in ZnO [16]. Consequently, for the non-polar ZnO film, because the *c*-axis lies in the growth plane, the anisotropic lateral growth rates of the grains along the two orthogonal directions lead to the stripe-like morphologies presented in the SEM images [17]. Non-polar GaN films also exhibit such anisotropic features [18]. Moreover, the low growth rate benefits for surface smoothness [19]. To further compare the surface roughness of *c*- and *m*-ZnO films, AFM measurements were performed. The 3D surface morphologies of *c*- and *m*-ZnO thin films are shown in Fig. 3(a)

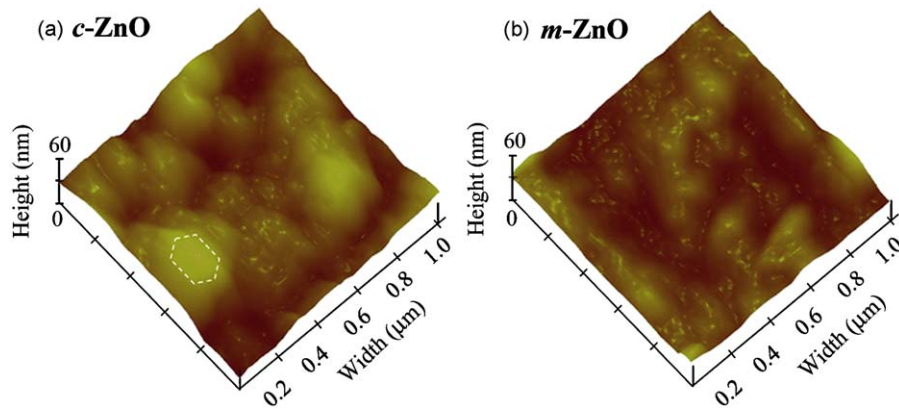


Fig. 3. (Color online) AFM images of the (a) *c*-plane and (b) *m*-plane ZnO thin films.

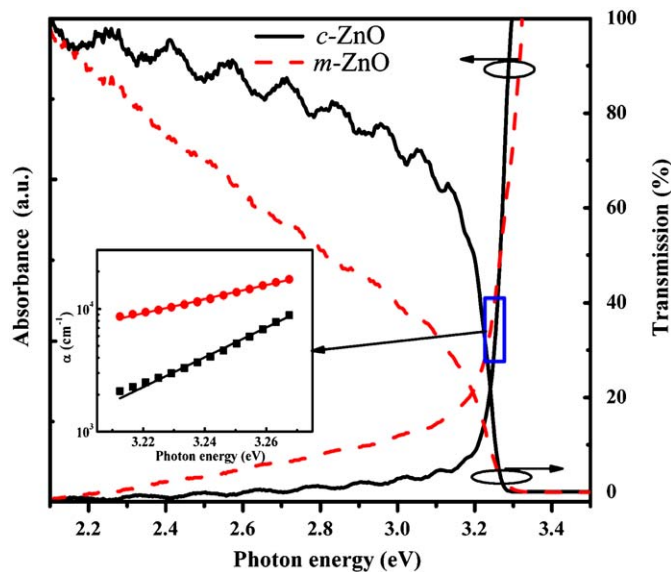


Fig. 4. (Color online) Optical absorption and transmission spectra of the *c*-plane and *m*-plane ZnO thin films, respectively. The inset shows absorption coefficient as a function of incident photon energy in near band-edge region.

and (b), respectively. Both samples were scanned in an area of $1 \times 1 \mu\text{m}^2$. There is obviously up-and-down surface on the *c*-ZnO film; somewhere hexagon-like grains can be seen. The *m*-ZnO film shows a smoother surface morphology than the *c*-ZnO film. The average surface roughness is determined to be 11 and 6 nm for the *c*- and *m*-ZnO films, respectively, confirming that the surface of the *m*-ZnO film is smoother than that of the *c*-ZnO film, in agreement with the SEM images.

Fig. 4 presents the optical absorption and transmission spectra of the *c*- and *m*-ZnO films. Sharp band edges of both samples are observed. However, comparing with the *c*-ZnO film, the *m*-ZnO film has a strong absorption in the band tails. A weak transmittance in the range of less than 3.2 eV is also observed in the transmission spectrum of *m*-ZnO film, in agreement with result obtained from the absorption spectrum. Generally, the band tail states are related to the presence of some defects [20–22]. The absorption coefficient of the *c*- and *m*-ZnO films as a function of the incident photon energy in the near band-edge region is shown in the inset in Fig. 4. We observed a large value of absorption coefficient achieved from *m*-ZnO thin film. The absorption coefficient can be expressed as follows according to Pankove's

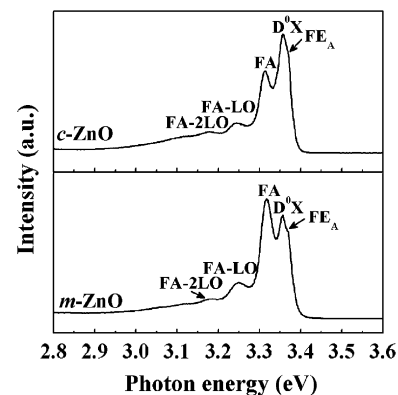


Fig. 5. PL spectra of the (a) *c*-plane and (b) *m*-plane ZnO thin films at 81 K.

description in the near band-edge regime:

$$\alpha(h\nu) = AE_0^{3/2} \exp\left[\frac{h\nu}{E_0}\right], \text{ for } h\nu < E_g, \quad (1)$$

where E_0 is an empirical parameter and usually weakly dependent on temperature [20]. Larger E_0 value represents more defects. In the present work, by fitting Eq. (1), the values E_0 are determined to be 36 and 77 meV for the *c*- and *m*-ZnO films, respectively. The fitting result indicates that the *m*-ZnO has higher defects density than the *c*-ZnO. The high defects density in the *m*-ZnO film is responsible for strong absorption in the band tails and may originate from the cross-hatched growth mode.

In order to study the effect of film orientation on photoluminescent properties of ZnO films, low-temperature PL measurements were performed. Fig. 5(a) and (b) presents the PL spectra of the *c*- and *m*-ZnO thin films at 81 K, respectively. Two strong PL peaks at 3.31 and 3.36 eV are observed for both ZnO films. The shoulder at high energy side is located at 3.37 eV, originating from the recombination of free-exciton (FE). The peak at 3.36 eV is due to the recombination of neutral-donor-bound-excitons (D^0X) [23]. Recently, the PL peak at 3.31 eV has been studied in detail by Schirra et al. [24]. The study indicates that the peak at 3.31 eV is ascribed to the transitions of conduction band electron to acceptors (FA) related to stacking faults in the ZnO films. To be brief, the origin of PL peaks at 3.31 and 3.36 eV is different, and the peak at 3.31 eV is related to acceptor defects but the peak at 3.36 eV is related to donor defects. The D^0X emission of the *c*-ZnO film is dominant but the FA emission of the *m*-ZnO film is strongest. It is suggested that the dominant defect type in the *c*-ZnO and *m*-ZnO is absolutely different. One possible

explanation is that the cross-hatched grains in the *m*-plane ZnO result in a great deal of grain boundaries where more stacking faults lead to strong 3.31 eV emissions.

Finally, it is well understood that the *c*- and *m*-ZnO films have large difference in the electron mobility. It is well known that mobility is strongly dependent on defect concentration and mechanism of scatterance. As mentioned above, the optical absorption spectroscopy and PL measurement indicate that the defect concentration of *m*-ZnO is higher than that of *c*-ZnO, which is responsible for low electron mobility. On the other hand, McLaurin and Speck found significant anisotropy in electron and hole mobility of heteroepitaxial *m*-plane GaN films with anisotropic distribution of stacking faults [25]. Similarly, the large electron mobility difference between *c*- and *m*-ZnO can be related to anisotropic distribution of stacking faults in the *m*-ZnO. As a result, the low electron mobility of the *m*-ZnO film is ascribed to the cross-hatched growth mode which produces more defects, such as stacking faults.

4. Conclusion

In conclusion, we have comparatively investigated the surface morphology, growth rate and optical properties of the polar and non-polar ZnO thin films. With respect to the polar *c*-ZnO film, the non-polar *m*-ZnO film has a smoother surface due to low growth rate. However, high defects density of the *m*-ZnO film result in strong band tail absorbance and 3.31 eV emissions as well as low mobility in electrical property.

Acknowledgements

This work was supported by the Key Project of National Natural Science Foundation of China under Grant no. 50532050, the “973” Program under Grant no. 2006CB604906, the Innovation Project of Chinese Academy of Sciences, and the National Natural Science Foundation of China under Grant nos. 60806002, 60506014, 10874178, 10674133, and 60776011.

References

- [1] Y.I. Alivov, E.V. Kalinina, A.E. Cherenkov, D.C. Look, B.M. Ataev, A.K. Omaev, M.V. Chukichev, D.M. Bagnall, Appl. Phys. Lett. 83 (2003) 4719.
- [2] D.C. Look, Mater. Sci. Eng., B 80 (2001) 383.
- [3] Y.I. Alivov, J.E. Van Nostrand, D.C. Look, M.V. Chukichev, D.M. Ataev, Appl. Phys. Lett. 83 (2003) 2943.
- [4] Y. Chen, D.M. Baghall, H. Koh, K. Park, K. Hiraga, Z. Zhu, T. Yao, J. Appl. Phys. 84 (1998) 3912.
- [5] S. Tian Jr., M.H. Liang, Y.T. Ho, Y.A. Liu, L. Chang, J. Cryst. Growth 310 (2008) 777.
- [6] A. Chakraborty, H. Xing, M.D. Craven, S. Keller, T. Mates, J.S. Speck, S.P. DenBaars, U.K. Mishra, J. Appl. Phys. 96 (4) (2004) 449.
- [7] F. Bernardini, V. Fiorentini, D. Vanderbilt, Phys. Rev. B 56 (1997) R10024.
- [8] X.L. Wu, G.G. Siu, C.L. Fu, H.C. Ong, Appl. Phys. Lett. 78 (2001) 2285.
- [9] J.M. Chauveau, D.A. Buella, M. Laugt, P. Vennegues, M. Teisseire Doninelli, S. Berard Bergery, C. Deparis, B. Lo, B. Vinter, C. Morhain, J. Cryst. Growth 301–302 (2007) 366.
- [10] C. Chen, V. Adivarahan, J. Yang, M. Shatalov, E. Kuokstis, M.A. Khan, Jpn. J. Appl. Phys., Part 1 42 (2003) 1039.
- [11] E. Cagin, J. Yang, W. Wang, J.D. Phillips, S.K. Hong, J.W. Lee, J.Y. Lee, Appl. Phys. Lett. 92 (2008) 233505.
- [12] J.Q. Xie, J.W. Dong, A. Osinsky, P.P. Chow, Y.W. Heo, S.J. Pearton, X.Y. Dong, C. Adelmann, C.J. Palmstrom. Progress in semiconductor materials V—novel materials and electronic and optoelectronic applications, MRS Symposia Proceedings No. 891, (Materials Research Society, Pittsburgh, (2006), p. 407.
- [13] N.W. Emanetoglu, J. Zhu, Y. Chen, J. Zhong, Y. Chen, Y. Lu, Appl. Phys. Lett. 85 (2004) 3702.
- [14] S.K. Han, S.K. Hong, J.W. Lee, J.Y. Lee, J.H. Song, Y.S. Nam, S.K. Chang, T. Minegishi, T. Yao, J. Cryst. Growth 309 (2007) 121.
- [15] T. Moriyama, S. Fujita, Jpn. J. Appl. Phys., Part 1 44 (2005) 7919.
- [16] X.C. Sun, H.Z. Zhang, J. Xu, Q. Zhao, R.M. Wang, D.P. Yu, Solid State Commun. 129 (2004) 803.
- [17] T.H. Huang, S.M. Zhou, H. Teng, H. Lin, J. Wang, P. Han, R. Zhang, J. Cryst. Growth 310 (2008) 3144.
- [18] P. Waltereit, O. Brandt, M. Ramsteiner, A. Trampert, H.T. Grahn, J. Menniger, M. Reiche, K.H. Ploog, J. Cryst. Growth 437 (2001) 227.
- [19] Toshihide Ide, Mitsuaki Shimizu, Jason Kuo, Kulandaive Jegannathan, Xu-Qiang Shen, Hajime Okumura, Phys. Status Solidi (c) 0 (7) (2003) 2549.
- [20] V. Srikant, D.R. Clarke, J. Appl. Phys. 81 (9) (1997) 6357.
- [21] D. Redfield, Phys. Rev. 130 (1963) 916.
- [22] D. Redfield, Phys. Rev. 140 (1963) A2056.
- [23] Ü. Özgür, Ya.I. Alivov, C. Liu, A. Teke, M.A. Reshchikov, S. Dogan, V. Avrutin, S.-J. Cho, H. Morkoç, J. Appl. Phys. 98 (2005) 041301.
- [24] M. Schirra, R. Schneider, A. Reiser, G.M. Prinz, M. Feneberg, J. Biskupek, U. Kaiser, C.E. Krill, K. Thonke, R. Sauer, Phys. Rev. B 77 (2008) 125215.
- [25] Melvin McLaurin, James S. Speck, Phys. Status Solidi (RRL) 1 (3) (2007) 110.